Identification of Talc and Chlorite Mineral in the Askot Crystalline of Kumaon Himalaya using Hyperion Hyperspectral data

H. Govil[1*] N. Gill[2] & S. Rajendran[3]

[1]*Department of Applied Geology, NIT Raipur, India (himgeo@gmail.com)*

[2]*Chhattisgarh Council of Science and Technology, Raipur (C.G.) India*

[3]*Department of Earth Sciences, Sultan Qaboos University, Al-Khod, 123 Muscat, Oman*

ABSTRACT:

In this study an EO-1 Hyperion hyperspectral data has been used to identify the talc and chlorite in the Askot crystallines of the Kumaon Himalaya near to the Ghattabagar village of the Askot town. Identification of the talc was done using the Hyperion data and results were verified by the field and laboratory analysis. Though the SNR of the Hyperion data was very low (10:1) but careful processing of the hyperspectral data has given a very good indication of talc and Chlorite mineral. VNIR and SWIR spectroscopy has been used effectively for identification of VNIR and SWIR active minerals. Mineralogy identified through the Hyperion data stands in good confirmation with the established geology of the area.

KEYWORDS: Hyperion hyperspectral data, Askot Crystallines, Spectroscopy, Talc mineral

1. INTRODUCTION:

Advent of space borne hyperspectral imagery has opened a new era of identification of hydrothermal alteration minerals through a remotely sensed data (Farooq and Govil, 2013). The EO-1 (earth observation) Hyperion is the only available space borne hyperspectral data available till today. The EO-1 was the part of NASA New Millennium Programme (NMP), which was created to flight-validate instrument and spacecraft technologies that could enable new or more cost-effective approaches to Earth observation. Both advanced multispectral imagers and hyperspectral imagers were part of the NMP Earth Observing-1 mission (Pearlman et al., 2003b; Ungar et al., 2003).

The Hyperion imaging spectrometer was the first spectrometer mounted on the NASA EO-1 satellite launched from Vandenburg Air Force Base on November 21, 2000 and is now in an orbit one minute behind Landsat 7 (Pearlman et al., 2003a). The EO-1 satellite contains three observing instruments supported by a variety of newly developed space technologies. The Hyperion Imaging Spectrometer is the first high spatial resolution imaging spectrometer in the orbit of the earth (Pearlman et al., 2003a; Ungar et al., 2003).

Hyperion has a single telescope and two spectrometers, one visible/near infrared (VNIR) spectrometer and the other shortwave infrared (SWIR) spectrometer. The telescope images the Earth onto a slit that defines the instantaneous field-of-view, which is 0.624° wide (i.e., 7.5 Km swath width from a 705 Km altitude) by 42.55 m radians (30 meters) in the satellite velocity direction. This slit image of the Earth is relayed at a magnification of 1.38:1 to two focal planes in the two grating imaging spectrometers. A dichroic filter in the system reflects the spectral region from 400 to 1,000 nm to the VNIR spectrometer and transmits the region from 900 to 2500 nm to the other SWIR spectrometer (Goodenough et al., 2003; Pearlman et al., 2003a; Pearlman et al., 2003b; Ungar et al., 2003).

In this study on demand Hyperion data was used to identify talc and other associated minerals near to the Askot area of the Pithoragarh district, Kumaon Himalaya, India. Askot area has its economic interest due to the availability of the basemetal minerals of the hydrothermal origin (Farooq, 1985; Farooq and Govil, 2013).

2. GEOLOGICAL SETTING OF THE STUDY AREA:

Crystallines are one of the most prominent and typical feature, occurring in the Kumaon and Garhwal Himalaya in the form of nappe and klippe.

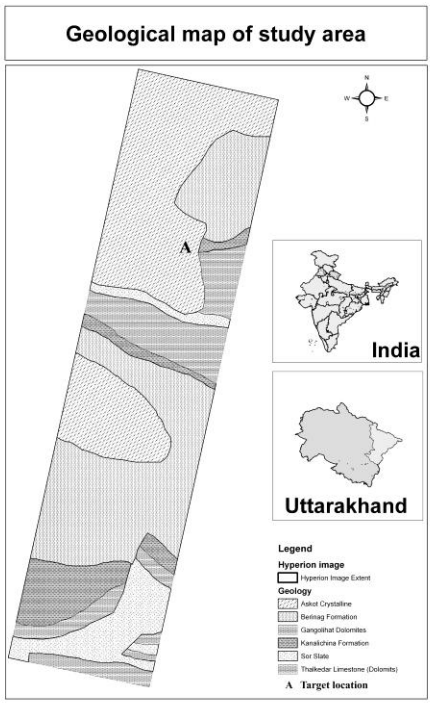

Figure 1: Geological map of the study area

The dominant rocks in the Askot crystallines are gneisses in the form of augen gneiss, granite gneiss, biotite-muscovite gneiss, calcsilicates and quartzites. Dikes of aplites and pegmatites are common in the rocks of higher (northern) horizons of this zone. The major rock types are gneisses, quartzites, variety of schists, calcsilicates, and leucogranite dikes especially at higher (northern) horizons (Bhattacharya, 2008)

3. HYPERSPECTRAL DATA PROCESSING:

The spectral sampling in the wavelength range of 2000-2500 nm is tailored to the needs of geologic mineral identification since the diagnostic spectral absorption features of altered minerals fall within this range. Extraction process included a sequential string of techniques (Mahoney et al., 2003), (Gersman.R. et al., 2008). Atmospheric correction, minimum noise fraction (MNF), pixel purity index (PPI), n-dimensional vizualizer and spectral angle mapper (SAM) allowed the discrimination of favorable alteration mineral assemblages and sites of potential mineralization. Figure 2 illustrates the various steps in data analysis.

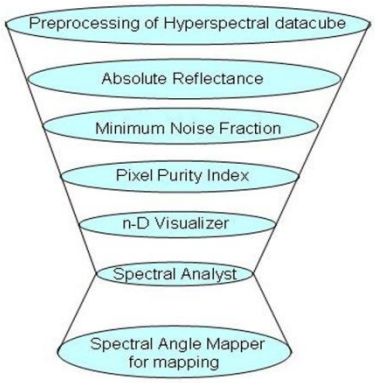

Figure 2: Methodology flow chart.

3.1 Preprocessing and Atmospheric Correction:

Band selection is most significant step for hyperspectral processing. Preprocessing of hyperspectral data helps select only the unique channels (9-57, 81-97, 101-119, 134-164 and 182-223) (Farooq and Govil, 2013; Jupp et al., 2004) and discard the overlapping and inactive channels. This selection leaves 158 unique channels for further processing. Visual examination of these 158 channels was done and 2 more channels were discarded due to the low signal to noise ratio and left 156 channels. Apart from the bands selection some other modifications like bad lines removal, first and last sample modification and VNIR and SWIR shift removal was done in the data cube. To remove the bad lines one code was written in the Iterative Data Language (IDL) which consider the before and after line to fill the bad lines.

Atmospheric correction using Fast Line-of-Sight Atmospheric Analysis of Spectral Hypercubes (FLAASH) developed on Moderate Resolution Atmospheric Radiance and Transmittance Model (MODTRAN) was implemented to convert radiance data to absolute reflectance in W m^{-2} sr^{-1} μm^{-1} (Anderson et al., 2000; Cairns et al., 2003; Envi, 2009; Kawishwar, 2007).

3.2. Data Dimensionality Reduction (MNF)

As suggested by Kruse (Kruse et al., 2003) the MNF rotation transform was applied in order to determine the inherent dimensionality of image data, to segregate noise and to reduce the computational requirements during subsequent processing. The image pixels are represented by eigenvalues, the dimensionality of the data was determined by examining these values (Green et al., 1988). It was observed that the first 15 bands have the highest eigenvalues (>1) while the

rest have values less than 1 (Figure.3). These low values are seen in the image as noise. The first 15 MNF bands were therefore selected for further processing.

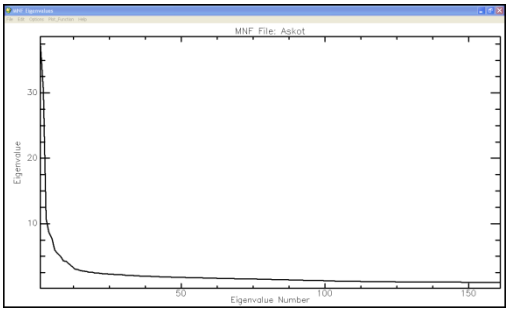

Figure.3: MNF Eigenvalues plot

3.3 Pixel Purity Index (PPI):

Pixel purity index is basically a function to identify the most spectrally pure pixels in the feature space of the available bands. This is computed by repeatedly projecting n-dimensional scatter plots on to a random unit vector and the number of times and projection of extreme pixel is recorded. Digital numbers of PPI image contain information corresponding to the number of times that pixel was recorded as extreme (Figure.4). The PPI image for the dataset under analysis was generated from the selected MNF bands.

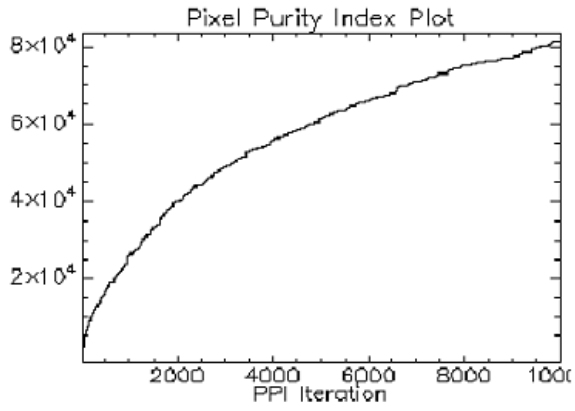

(a) **(b)**

Figure.4: (a) Pixel Purity Image, (b) PPI Plot

3.4. n-Dimensional Visualizer

n-dimensional visualizer is a function used to identify the purest pixels and most extreme spectral responses in the multidimensional feature space of hyperspectral datasets. This assists in visualizing the extreme pixel and identifying and selecting that pixel as an endmember for further classification and map generation. N-dimensional visualizer was used to identify the purest pixel within in the subset (Figure.5). A total two purest pixel of talc and chlorite (Figure.6) were identified for classification. The spectral analyst function in ENVI was used to identify the pure pixels by comparing their spectra with the USGS spectral library.

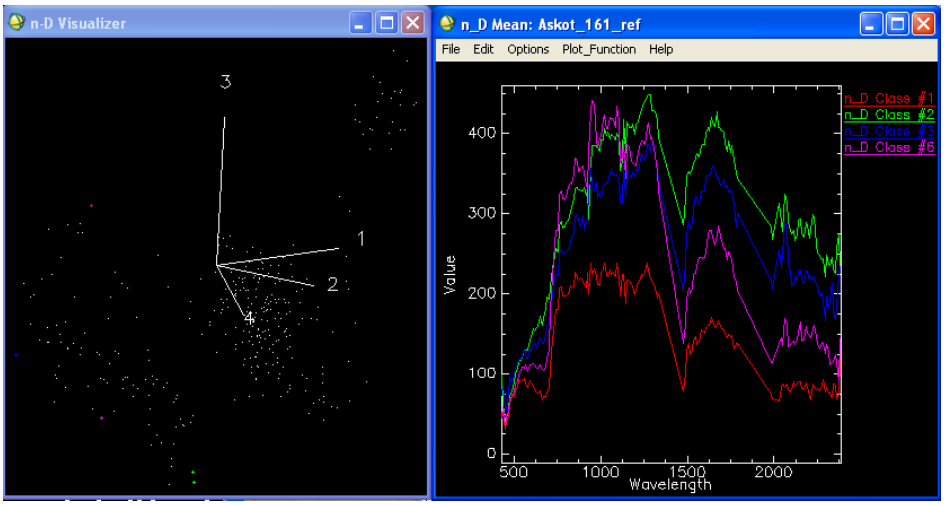

(a) **(b)**

Figure.5: (a) n-dimensional visualizer (b) Endmembers spectra

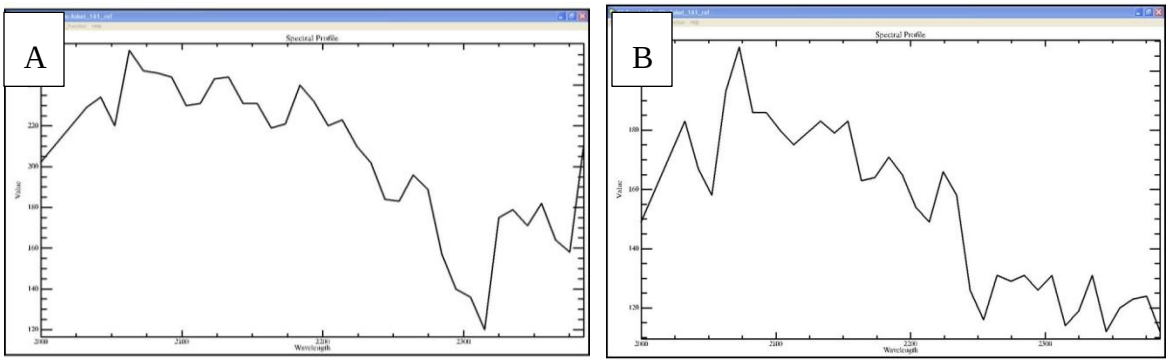

Figure.6: Hyperion spectral signature of the Talc and Clinochlore minerals

3.5. Spectral Angle Mapper (SAM)

This is a physically based image classification which uses an n-dimensional angle to match image spectra with the reference spectra. SAM calculates the angle between the spectra and treats them as vectors in a space with dimensionality equal to the number of bands.

Two separate mineral maps for Talc and Chlorite using SAM were generated. These maps were used to identify targets for detailed field investigations. Figure 6 shows the mineral maps of the study area.

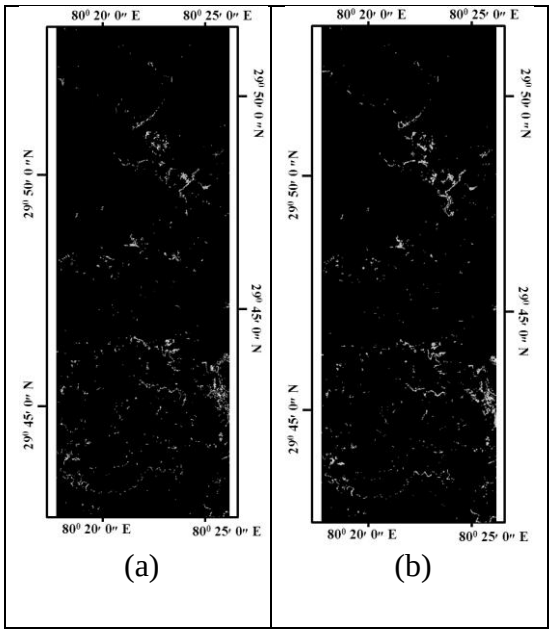

Figure.6: Mineral map of the study area (a) Talc ((d) Chlorite

4. RESULTS:

On the basis of the mineral map prepared by the spectral angle mapper classification a field investigation was conducted to check the results. Location "A" on the map Figure.1 was found as a Ghattabagar village near the right bank of the Gori river in the NE direction of the Askot area. This location is barely 2 km away in the SW direction from the Patoli Nala village. Here, a big mining area of hydrothermal talc has been found which was not known to the investigator before and was identified only with the help of Hyperion data

The host rock in this area is the augen gneisses in which quartz porphyroblasts are unreplaced and the matrix is completely replaced by the talcose minerals (Figure 7a). Here the talc is occurring in the pure white colored, fine grained laminated rock trending in NNW SSE with dip 80 NE in a renderedly schistose rock. A gossanised capping over the talcose rock has been identified, where lower portion of the rock remained intact. Laminated iron formation has also been identified within the pure talc as bands at different locations (Figure 7b).

Talc ($Mg_3Si_4O_{10}(OH)_2$) is a phyllosilicate and crystallize in the monoclinic system. It is a product of low grade regional metamorphism of magnesium rich minerals like dolomite, pyroxenite, serpentinite, chlorite schists etc. It also occurs in association with Serpentinisation (Gribble, 1991).

Talc is also a SWIR active mineral, which exhibits its diagnostic absorption feature at 2315nm accompanying shoulder absorption feature at 2285nm and 2245nm along with a small absorption feature at 2386nm, due to the vibrational process, which is responsible for the MgOH. OH and H-O-H absorption features in the talc occur at 1393nm and 1905nm. Figure 7c illustrates the talc spectra of the samples collected from the Ghattabagar village near the Askot town which contains the diagnostic absorption Talc mineral. Fe^{2+}/Fe^{3+} absorption feature has been observed near to 1000nm due to crystal field absorption of Fe^{2+} (King and Ridley, 1987).

Clinochlore ($(Mg, Fe^{++})_5Al(Si_3Al)O_{10}(OH)_8$) is a phyllosilicate, comes under the category of Chlorite group and crystallize in the monoclinic system. It occurs as a primary mineral in low grade regional metamorphic rock and as a secondary mineral forming from hydrothermally breakdown of pyroxene, amphibole and biotite (Gribble, 1991).

Clinochlore is a SWIR active mineral and shows diagnostic absorption features at 2255nm and 2315-2345nm, which is due to the presence of AlFe-OH or AlMg-OH and MgOH vibrational process (Bishop et al., 2008). OH and H-O-H absorption features occur at 1393nm and 1995nm. Some additional bands also occur between 2400-2500nm. These bands are probably due to the OH stretching and bending combinations (Bishop J.L. et al., 2002; Gates W.P., 2005). Figure 7d represent the Ghattabagar area spectral signatures. These spectra are the mixture of Talc and Clinochlore. Apart from all the diagnostic absorption features of the Clinochlore, it also exhibits absorption of the talc mineral from 2075-2235nm.

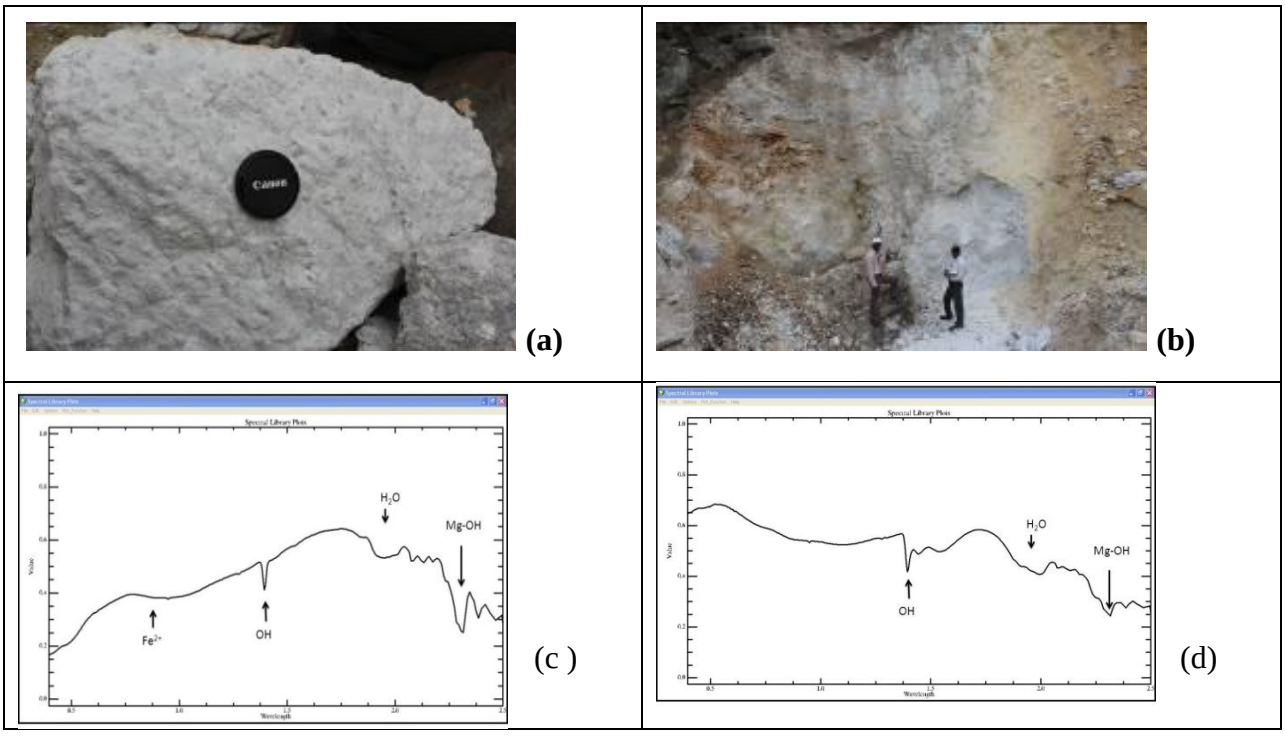

Figure.7: Laboratory spectral signature of the Talc and Clinochlore minerals

5. DISCUSSION AND CONCLUSION:

The most prominent indications of rock alteration/weathering in the Ghattabagar site are: rich goethite mineral coverage over the thickly bedded talcose rocks, alteration of gneisses into chloritic talc, white gneisses alteration into the chloritic matrix with unreplaced quartz, surface bleaching and discoloration of country rock. Fe rich talc bands, which were renderedly schistose, have been found in between the pure white talc. Pyrite has also been discovered from the mining area. Brown and yellow colors of rocks are due to the hydrous oxides originating by the decomposition of the pyrite. The major alteration type, recognized in the Ghattabagar site is the talc alteration.

A careful analysis of the Hyperion image with the established procedures coupled with

the laboratory analysis of the rock samples allowed the researchers to identify the talc mineralization in the rugged terrain of the Kumaon Himalaya. The mineralogy identified through the Hyperion images is largely consistent with the established geology of the study area. Though the SNR of the Hyperion image was very low but still the data was able to give a clear identification of the talc and chlorite in the study area. VNIR region of the field samples were helpful to identify the Goethite mineral. SWIR region of the rock spectrum was effectively used to identify the SWIR active minerals viz. Talc and Clinochlore. In short spectroscopy has been proven a good technique to identify the talc and Clinochlore minerals in the rugged terrain of the Kumaon Himalaya.

6. REFERENCES:

Anderson, G.P., Berk, A., Acharya, P.K., Matthew, M.W., Bernstein, L.S., Chetwynd, J.H., Dothe, H., Adler-Golden, S.M., Ratkowski, A.J., Felde, G.W., Gardner, J.A., Hoke, M.L., Richtsmeier, S.C., Pukall, B., Mello, J., Jeong, L.S., 2000. MODTRAN4: Radiative Transfer Modeling for Remote Sensing. SPIE 4049, 176-183.

Bhanot, V.B., Pandey, B.K., Singh, V.P., Thakur, V.C., 1977. Rb-Sr whole rock age of the granitic-gneisses from Askote area, eastern Kumaon and its implications on tectonics interpretation of the area. Himalayan Geology 7, 118-122.

Bhattacharya, A.R., 1980. New light on the stratigraphy and structure of the Kumaon lesser Himalaya: A study in mathmatical perspective. Today and Tomorrow's Printers & Publishers.

Bhattacharya, A.R., 2008. Basement Rocks of the Kumaun - Garhwal Himalaya: Implications for Himalayan Tectonics. Earth Science India 1, 1-10.

Bishop J.L., Murad E., M.D., D., 2002. The influence of octahedral and tetrahedral cation substitution on the structure of smectites and serpentines as observed through infrared spectroscopy. Clay Minerals, 617-628.

Bishop, J.L., Lane, M.D., Dyar, M.D., Brown, A.J., 2008. Reflectance and emission spectroscopy study of four groups of phyllosilicates: smectites, kaolinite-serpentines, chlorites and micas. Clay Minerals 43, 35-54.

Cairns, B., Carlson, B.E., Ying, R.X., Lacis, A.A., Oinas, V., 2003. Atmospheric correction and its application to an analysis of Hyperion data. IEEE Transactions on Geoscience and Remote Sensing 41, 1232-1245.

Envi, 2009. Atmospheric correction module: QUAC and FLAASH user's guide.

Farooq, S., 1985. Basemetal Mineralization in Askote Area, Pithoragarh Distt., Kumaon Himalaya, Geology. Aligarh Muslim Univeristy, Aligarh, p. 145.

Farooq, S., Govil, H., 2013. Mapping Regolith and Gossan for Mineral Exploration in the Eastern Kumaon Himalaya, India using hyperion data and object oriented image classification. Advances in Space Research 53, 1676-1685.

Gansser, A., 1964. Geology of the Himalayas. Intersci. Pub., London.

Gates W.P., 2005. Infrared spectroscopy and the chemistry of dioctahedral smectites. The Clay Minerals Society, Aurora, Colorado, USA.

Gersman.R., Ben-Dor, E., Beyth, M., Avigad, D., Abraha, M., Kibreab., A., 2008. Mapping of hydrothermally altered rocks by the EO-1 Hyperion sensor, Northern Denakil Depression, Eriteria. International Journal of Remote Sensing 29, 3911-3936.

Ghose, A., Chakraborti, B., Singh, R.K., 1974. Structure and metamorphic history of the Almora group, Kumaon Himalaya, Uttar Pradesh. Himalayan Geology 4, 171-194.

Goodenough, G.D., Dyk, A., Niemann, O.K., Pearlman, J.S., 2003. Preprocessing Hyperion and ALI for forest classification. IEEE Transactions on Geoscience and Remote Sensing 41, 1321-1331.

Green, A.A., Berman, M., Switzer, P., Craig, M.D., 1988. A transformation for ordering multispectral data in terms of image quality with implications for noise removal. IEEE Transactions on Geoscience and Remote Sensing 26, 65-74.

Gribble, C.D., 1991. Rutley's elements of minerology, 27th ed. CBS Publishers and distributors, Delhi.

Heim, A., Gansser, A., 1939. Central Himalaya, geological observations of the Swiss expendition 1936. Hindustan Publishing Corporation (India).

Jupp, D.L.B., Datt., B., Lovell, J., Campbell, S., King, E., 2004. Background notes for Hyperion data user workshop. CSIRO office of space science and applications, Earth Obersvation Centre.

Kawishwar, P., 2007. Atmospheric Correction Models for Retrievals of Calibrated Spectral Profile from Hyperion EO1 data Geoinformatics. ITC and IIRS, Netherlands & Dehradun, p. 84.

King, T.V.V., Ridley, W.I., 1987. Relation of the Spectroscopic Reflectance of Olivine to Mineral Chemistry and Some Remote Sensing Implications. J. Geophys. Res., 11457-11469.

Kruse, F.A., Boardman, J.W., Huntigton, J.F., 2003. Comparison of airborne hyperspectral data and EO-1 Hyperion for mineral mapping. IEEE Transactions on Geoscience and Remote Sensing 41, 1388-1400.

Mahoney, S., James, P., Mauger, A., Heinson, G., 2003. Geologic and regolith mapping for mineral exploration in the Gawlter Craton of South Australia using Hyperion and other remote sensing techniques, Geoscience and Remote Sensing Symposium, pp. 1779-1781.

Misra, R.C., Bhattacharya, A.R., 1976. The Central Crystalline zone of northern Kumaon Himalaya: Its lithostratigraphy, structure and tectonics with special reference to plate tectonics. Himalayan Geology 3, 320-335.

Misra, R.C., Sharma, R., 1972. Structure of Almora Crystallines, Lesser Kumaon Himalaya: An interpretation. Himalayan Geology 2, 330-341.

Misra, R.C., Sharma, R., Sinha, A.K., 1973. Petrochemistry of the Almora Crystalline, Kumaon Himalaya. Himalayan Geology 3, 411-435.

Pearlman, J., Carman, S., Segal, C., Jarecke, P., Barry, P., 2003a. EO1 Overview of the Hyperion Imaging Spectrometer for the NASA EO-1 Mission. NASA.

Pearlman, J.S., Barry, P.S., Segal, C.C., Shepanski, J., Beiso, D., Carman, S.L., 2003b. Hyperion, a space-based imaging spectrometer. IEEE Transactions on Geoscience and Remote Sensing 41, 1160-1173.

Saxena, S.P., 1974. Geology of the Marchula-Bhikiasen area, district Almora, Uttar Pradesh with special reference to south Almora Thrust. Himalayan Geology 4, 630-647.

Saxena, S.P., Rao, P.N., 1975. Dose Almora Nappe exist? Himalayan Geology 5, 169-184.

Ungar, S.G., Pearlman, J.S., Mendenhall, J.A., Reuter, D., 2003. Overview of the Earth Observing One (EO-1) mission. IEEE Transactions on Geoscience and Remote Sensing 41, 1149-1159.